Available online at www.sciencedirect.com
SCIENCE DIRECT®
European Journal of Mechanics B/Fluids 21 (2002) 739–750

Curvature effects on the surface viscosity of nematic liquid crystals

Paolo Biscari [a,b]

[a] *Dipartimento di Matematica, Politecnico, Piazza Leonardo da Vinci 32, 20133 Milano, Italy*
[b] *Istituto Nazionale di Fisica della Materia, Via Ferrata 1, 27100 Pavia, Italy*

Received 18 March 2002; accepted 11 September 2002

Abstract

We analyse the flow of a nematic liquid crystal close to a cylindrical surface. As a first result, we show that it is not possible to decouple the motion equations for the director and the macroscopic velocity. Nevertheless, we derive an expression for an effective viscosity, which can be used in the dynamic boundary condition linking the time derivative and the gradient of the director angle on the surface. The effective viscosity so obtained may be greater or smaller than its planar counterpart, depending on both the concavity of the surface and the sign of the Leslie coefficients α_2 and α_3. In particular, in materials that align in shear, the correction to the surface viscosity changes sign depending on whether the angle between the director and the surface normal exceeds or not a critical value.

PACS: 61.30.Hn; 68.10.Et

MSC: 76A15; 76D10

1. Introduction

Nematic liquid crystals are anisotropic fluids, composed by elongated molecules which possess head-and-tail symmetry. Their configuration may be described by assigning at each point the *director*, that is, a vector $\mathbf{n} \in \mathbb{S}^2$ parallel to the local molecular direction. The inversion symmetry which characterizes the nematic molecules implies that all constitutive equations describing a nematic sample must be symmetric under the reflection $\mathbf{n} \leftrightarrow -\mathbf{n}$.

The bulk equations governing the flow of a nematic liquid crystal, first derived by Ericksen [1,2] and Leslie [3], are able to describe in a satisfactory way the dynamics of a defect-free material away from the boundary. Much effort has been made in order to determine the correct dynamic boundary conditions to be imposed on a flowing nematic liquid crystal. Rapini and Papoular [4] proposed the first static model for the treatment of nematic boundaries. Some years later, the first time-dependent boundary condition was proposed by Pikin et al. [5], and then Derzhanski and Petrov [6] put forward a systematic theory involving a surface viscosity $h\,\gamma_{\rm s}$, where h is a length and $\gamma_{\rm s}$ a bulk viscosity, to be introduced in the phenomenological dynamic boundary condition

$$h\,\gamma_{\rm s}\,\dot{\vartheta}_{\rm s} = K\,\vartheta'_{\rm s} + \mathbb{K}_{\rm s}. \tag{1.1}$$

In (1.1), $\vartheta_{\rm s}$ denotes the angle between the surface director and the normal to the surface, K is an average elastic constant, and $\mathbb{K}_{\rm s}$ is the torque exerted by the surface. The boundary condition (1.1) has been widely used thenceforth [7–11]. Recent measurements [12] have estimated h in the range of 10 nm, even if the characteristic surface relaxation time which would

E-mail address: paolo.biscari@polimi.it (P. Biscari).

0997-7546/02/$ – see front matter
PII: S0997-7546(02)01213-X

be associated with such a surface length is in partial disagreement with the fast switching times involved in surface bistable devices [13,14].

Durand and Virga [15] have illustrated a possible hydrodynamic origin of the phenomenological boundary condition (1.1). They hypothesize the existence of a *boundary layer*, where the surface orienting field is diluted, and study the planar flow of a nematic liquid crystal bounded by an infinite plane. In this setting, and applying Ericksen–Leslie theory, they prove that $\dot\vartheta$, the time-derivative of the director angle, and v', the flow gradient, are related to the elastic and surface specific torques through:

$$\dot\vartheta = \frac{K\vartheta'' + K_{\mathrm{s}}}{\gamma_{\mathrm{s}}(\vartheta)} \quad \text{and} \quad \frac{v'}{2} = \left(\frac{\gamma_1}{\gamma_{\mathrm{s}}(\vartheta)} - 1\right)\frac{K\vartheta'' + K_{\mathrm{s}}}{\gamma_1 - \gamma_2\cos 2\vartheta}. \tag{1.2}$$

In (1.2), the *effective viscosity* γ_{s} is defined as

$$\gamma_{\mathrm{s}}(\vartheta) := \gamma_1 - 2\,\frac{g^2(\vartheta)}{f(\vartheta)}, \tag{1.3}$$

with

$$\begin{aligned} f(\vartheta) &:= 2\alpha_1 \sin^2\vartheta\cos^2\vartheta + \alpha_4 + (\alpha_5 - \alpha_2)\cos^2\vartheta + (\alpha_6 + \alpha_3)\sin^2\vartheta \quad \text{and} \\ g(\vartheta) &:= \alpha_2\cos^2\vartheta - \alpha_3\sin^2\vartheta. \end{aligned} \tag{1.4}$$

The material coefficients $\{\alpha_1, \ldots, \alpha_6\}$ are the Leslie coefficients, while $\gamma_1 := \alpha_3 - \alpha_2$ and $\gamma_2 := \alpha_6 - \alpha_5$. An effective viscosity alike (1.3), arising from the separability of the equations for flow and molecular orientation, was first introduced by Van Doorn [16], and then used in [17].

The field equations (1.2), when integrated across the boundary layer (of width h), yield to (1.1), and give a physical meaning to the phenomenological quantities introduced therein. In particular, Eq. (1.3) shows that the effective viscosity to be introduced in the boundary condition (1.1) depends on the director orientation.

In this paper, we generalize the analysis of [15] to study the flow of a nematic liquid crystal bounded by a curved surface. We derive the motion equations for the director and the macroscopic velocity, valid both in the bulk and close to the boundary, and compare different classes of special solutions, in order to highlight the motions most influenced by the curvature of the boundary. We find that the curved surface influences the motion equations only when the normal to the surface varies along the stream lines, that is when $(\nabla_{\mathrm{s}}\boldsymbol{\nu})\mathbf{v}$ is not null, where $\nabla_{\mathrm{s}}\boldsymbol{\nu}$ denotes the surface gradient of the normal unit vector.

Furthermore, we prove that the phenomenological boundary condition (1.1) can still be used, provided we modify properly the definition of γ_{s}, to take into account the curvature effects. In fact, the surface viscosity depends not only on the director direction, but also on the curvature and the concavity of the bounding surface. The sign of the curvature corrections is not fixed. In particular, for materials that align in shear, it changes when the angle between the director and the unit normal crosses a critical value, which depends on the degree of orientation of the nematic.

The plan of the paper is as follows. In Section 2 we briefly recall the Ericksen–Leslie theory of nematic flows. Section 3 specializes the preceding field equations to the case of a nematic flowing around a cylindrical surface. In Section 4 some special solutions of the field equations are studied, in order to highlight the particular motions in which the curvature effects are more tangible. In Section 5 we integrate the field equations over the boundary layer, and we derive the dynamic boundary condition to be imposed on a nematic liquid crystal flowing close to a curved surface. We retrieve an equation similar to (1.1), with an effective viscosity modified by the curvature of the boundary. Finally, in Section 6 we summarize the main results obtained in this paper.

2. Balance equations

The dynamic balance equations of the forces and the torques applied in the bulk of a nematic liquid crystal have been derived by Ericksen [1,2] and Leslie [3]. In both equations, we will as usual neglect molecular as well as rotational inertia.

In the absence of external fields (other than the field induced by the surface), the balance of forces reduces to

$$-\nabla W_{\mathrm{s}} + \operatorname{div}\mathbf{T} = \mathbf{0}, \tag{2.1}$$

where W_{s} is the surface potential energy. The stress tensor can be decomposed in an elastic and a viscous part: $\mathbf{T} = \mathbf{T}_{\mathrm{e}} + \mathbf{T}_{\mathrm{v}}$, with

$$\begin{aligned} \mathbf{T}_{\mathrm{e}} &= -p\mathbf{I} - (\nabla\mathbf{n})^{\mathrm{T}}\left(\frac{\partial W_{\mathrm{e}}}{\partial\nabla\mathbf{n}}\right) \quad \text{and} \\ \mathbf{T}_{\mathrm{v}} &= \alpha_1\big(\mathbf{n}\cdot(\operatorname{sym}\nabla\mathbf{v})\mathbf{n}\big)\mathbf{n}\otimes\mathbf{n} + \alpha_2\boldsymbol{\omega}\wedge\mathbf{n}\otimes\mathbf{n} + \alpha_3\,\mathbf{n}\otimes\boldsymbol{\omega}\wedge\mathbf{n} + \alpha_4\operatorname{sym}\nabla\mathbf{v} + \alpha_5(\operatorname{sym}\nabla\mathbf{v})\mathbf{n}\otimes\mathbf{n} \\ &\quad + \alpha_6\,\mathbf{n}\otimes(\operatorname{sym}\nabla\mathbf{v})\mathbf{n}. \end{aligned} \tag{2.2}$$

In (2.2), p is the hydrostatic pressure, $\mathbf{n}$ denotes the director field, $\mathbf{v}$ is the macroscopic fluid velocity, W_{e} is the elastic free energy density of the liquid crystal [18], and $\boldsymbol{\omega}$ is the angular velocity of the director relative to the fluid:

$$\boldsymbol{\omega} = \mathbf{w} - \frac{1}{2}\operatorname{rot}\mathbf{v}, \quad \text{with } \dot{\mathbf{n}} = \mathbf{w} \wedge \mathbf{n}.$$

We remark that the elastic part of the stress tensor may fail to be symmetric, even if it turns out to be so in the context of the one-constant approximation we will apply below. The viscous part $\mathbf{T}_{\mathrm{V}}$ could be symmetric only if both $\alpha_2 = \alpha_3$ and $\alpha_5 = \alpha_6$; we will show in Section 5 that most liquid crystal materials do not obey to these conditions.

The balance of torques requires the elastic, the viscous and the surface torques to be equilibrated:

$$\mathbf{K}_{\mathrm{e}} + \mathbf{K}_{\mathrm{V}} + \mathbf{K}_{\mathrm{S}} = \mathbf{0}, \tag{2.3}$$

where:

$$\mathbf{K}_{\mathrm{e}} = \mathbf{n} \wedge \left(\operatorname{div}\left(\frac{\partial W_{\mathrm{e}}}{\partial \nabla \mathbf{n}}\right) - \frac{\partial W_{\mathrm{e}}}{\partial \mathbf{n}}\right), \quad \mathbf{K}_{\mathrm{V}} = -\gamma_1 \boldsymbol{\omega} - \gamma_2\, \mathbf{n} \wedge (\operatorname{sym} \nabla \mathbf{v})\, \mathbf{n}, \quad \text{and} \quad \mathbf{K}_{\mathrm{S}} = -\mathbf{n} \wedge \frac{\partial W_{\mathrm{S}}}{\partial \mathbf{n}}. \tag{2.4}$$

Clearly, $\mathbf{K}_{\mathrm{S}}$ is expected to be significantly different from zero only close to the boundary. In (2.4) we have supposed that $\boldsymbol{\omega} \cdot \mathbf{n} = 0$. This can always be assumed, since the angular velocity $\mathbf{w}$ is defined up to an additive term of the type $\lambda\mathbf{n}$, and it always exists a λ that makes $\boldsymbol{\omega}$ orthogonal to $\mathbf{n}$.

2.1. Parametrization

We want to apply the balance equations (2.1) and (2.3) to study the flow of a liquid crystal close to a cylindrical surface. To this aim, and introducing the orthonormal basis $\{\mathbf{e}_r, \mathbf{e}_\varphi, \mathbf{e}_z\}$ shown in Fig. 1, we write

$$\begin{aligned} &\mathbf{n} = \cos\xi(t,r)\cos\vartheta(t,r)\,\mathbf{e}_r + \cos\xi(t,r)\sin\vartheta(t,r)\,\mathbf{e}_\varphi + \sin\xi(t,r)\,\mathbf{e}_z \quad \text{and} \\ &\mathbf{v} = v_r(t,r)\,\mathbf{e}_r + v_\varphi(t,r)\,\mathbf{e}_\varphi + v_z(t,r)\,\mathbf{e}_z. \end{aligned} \tag{2.5}$$

Thus, we assume that radial as well as translational symmetry along the axis of the cylinder exists. The director $\mathbf{n}$ is orthogonal to $\mathbf{e}_z$ when $\xi = 0$, orthogonal to $\mathbf{e}_\varphi$ when $\vartheta = 0$, and orthogonal to $\mathbf{e}_r$ when $\vartheta = \pi/2$; it is parallel to $\mathbf{e}_z$ when $\xi = \pi/2$.

The equation of continuity of the incompressible fluid restricts the values $\mathbf{v}$ may attain:

$$\operatorname{div}\mathbf{v} = v_r' + \frac{v_r}{r} \equiv 0 \quad \forall r \quad \Rightarrow \quad v_r(t,r) = \frac{R_0(t)}{r} v_0(t). \tag{2.6}$$

Furthermore, if the fluid is bounded by either an inner or an outer cylindrical surface of radius R, the normal component of the velocity must vanish at the boundary: $v_r(t,R) = 0$, and so, by (2.6), $v_r(t,r) \equiv 0$ for all t and r.

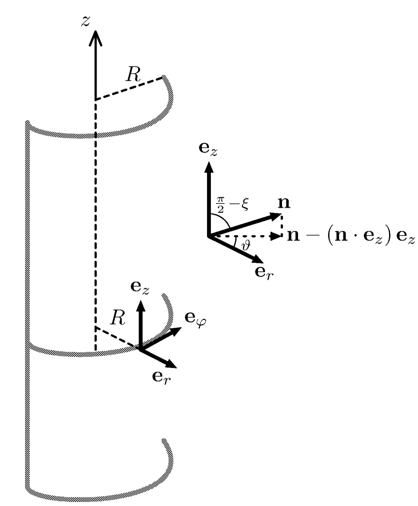

Fig. 1. Geometrical setting fit to describe the flow close to a cylindrical surface. The director $\mathbf{n}$ determines an angle ξ with the plane orthogonal to $\mathbf{e}_z$, while ϑ is the angle between the projection of $\mathbf{n}$ in the same plane and the radial unit vector $\mathbf{e}_r$.

When the nematic flows around a cylindrical surface, curvature effects are expected to be more tangible when the unit normal varies along the stream lines. In cylindrical coordinates, the unit normal $\boldsymbol{\nu}$ coincides with the radial unit vector $\mathbf{e}_r$, and thus

$$(\nabla_{\mathrm{s}}\boldsymbol{\nu})\mathbf{v} := \big[(\mathbf{I}-\mathbf{e}_r\otimes\mathbf{e}_r)\nabla\mathbf{e}_r\big]\mathbf{v} = \frac{1}{r}(\mathbf{e}_\varphi\otimes\mathbf{e}_\varphi)\,\mathbf{v} = \frac{v_\varphi}{r}\,\mathbf{e}_\varphi.$$

In fact, we will show in Section 4 below that the motion equations are sensibly different from their planar counterparts when the material flows tangentially around the external surface.

2.2. Elastic energy

In the following, and in order to better compare our results with those illustrated in the Introduction, we will use the one-constant approximation for the elastic potential:

$$W_{\mathrm{e}}(\mathbf{n},\nabla\mathbf{n}) = \frac{K}{2}|\nabla\mathbf{n}|^2 = \frac{K}{2}\left(\xi'^2+\frac{\cos^2\xi}{r^2}+\cos^2\xi\,\vartheta'^2\right),$$

where a prime denotes differentiation with respect to the radial variable. As a consequence,

$$\mathbf{T}_{\mathrm{e}} = -p\mathbf{I} - K(\nabla\mathbf{n})^{\mathrm{T}}(\nabla\mathbf{n}) \quad \text{and} \quad \mathbf{K}_{\mathrm{e}} = K\,\mathbf{n}\wedge\Delta\mathbf{n}.$$

2.3. Surface potential energy

We will assume that the concentrated surface torques are replaced by a surface potential energy W_{s}, diluted in a thin layer close to the boundary [19,20]. In order to describe both homeotropic and planar anchoring, we assume the following functional form for W_{s}:

$$W_{\mathrm{s}}(\mathbf{n},r) := \frac{1}{2}\,W_{\mathrm{s}r}(r)\,(\mathbf{n}\cdot\mathbf{e}_r)^2 + \frac{1}{2}W_{\mathrm{s}z}(r)(\mathbf{n}\cdot\mathbf{e}_z)^2. \tag{2.7}$$

The potential energy (2.7) has been introduced in [21] as a generalization of the expression previously proposed by Rapini and Papoular [4]. Independently of the dilution laws $W_{\mathrm{s}r}(r)$ and $W_{\mathrm{s}z}(r)$, W_{s} is stationary with respect to $\mathbf{n}$ when the director is directed along any of the three unit vectors $\mathbf{e}_r$, $\mathbf{e}_\varphi$, or $\mathbf{e}_z$. Homeotropic anchoring is enforced on the surface if $W_{\mathrm{s}r}\leqslant W_{\mathrm{s}z}$ and $W_{\mathrm{s}r}\leqslant 0$. The preferred direction is $\mathbf{e}_z$ if $W_{\mathrm{s}z}\leqslant W_{\mathrm{s}r}$ and $W_{\mathrm{s}z}\leqslant 0$. Finally, W_{s} pushes towards the tangential direction $\mathbf{e}_\varphi$ if both $W_{\mathrm{s}r}$ and $W_{\mathrm{s}z}$ are positive.

With the proposed surface potential energy, the *molecular field* $\mathbf{H}_{\mathrm{s}}$, acting on the nematic close to the boundary, is given by

$$\mathbf{H}_{\mathrm{s}} := -\frac{\partial W_{\mathrm{s}}}{\partial\mathbf{n}} = -W_{\mathrm{s}r}\cos\xi\cos\vartheta\,\mathbf{e}_r - W_{\mathrm{s}z}\sin\xi\,\mathbf{e}_z.$$

3. Flow around a cylinder

By using the parametrization (2.5), it is possible to write the angular velocity of the director as

$$\mathbf{w} = \lambda\,\mathbf{n} - \dot\xi\,\mathbf{n}_\parallel + \dot\vartheta\cos\xi\,\mathbf{n}_\perp,$$

provided we define the unit vectors $\mathbf{n}_\parallel := -\sin\vartheta\,\mathbf{e}_r + \cos\vartheta\,\mathbf{e}_\varphi$ and $\mathbf{n}_\perp := \mathbf{n}\wedge\mathbf{n}_\parallel$ that, together with $\mathbf{n}$, complete an orthonormal basis. Furthermore, and assuming from now on that $v_r(t,r)\equiv 0$ because of the equation of continuity of the fluid, we have:

$$\nabla\mathbf{v} = -\frac{v_\varphi}{r}\,\mathbf{e}_r\otimes\mathbf{e}_\varphi + v_\varphi'\,\mathbf{e}_\varphi\otimes\mathbf{e}_r + v_z'\,\mathbf{e}_z\otimes\mathbf{e}_r.$$

In particular,

$$\begin{aligned}\operatorname{rot}\mathbf{v} &= -v_z'\,\mathbf{e}_\varphi + \left(v_\varphi' + \frac{v_\varphi}{r}\right)\mathbf{e}_z\\ &= \left[\sin\xi\left(v_\varphi'+\frac{v_\varphi}{r}\right) - v_z'\sin\vartheta\cos\xi\right]\mathbf{n} - v_z'\cos\vartheta\,\mathbf{n}_\parallel + \left[\cos\xi\left(v_\varphi'+\frac{v_\varphi}{r}\right) + v_z'\sin\vartheta\sin\xi\right]\mathbf{n}_\perp.\end{aligned}$$

Finally, as we announced above, we determine λ in order to guarantee that $\boldsymbol{\omega}\cdot\mathbf{n}=0$. This yields:

$$\lambda = \frac{1}{2}\operatorname{rot}\mathbf{v}\cdot\mathbf{n} = \frac{\sin\xi}{2}\left(v_\varphi'+\frac{v_\varphi}{r}\right) - \sin\vartheta\cos\xi\,\frac{v_z'}{2}.$$

3.1. Balance of torques

If we now replace the above expressions in (2.4), we obtain:

$$
\begin{aligned}
\mathbf{K}_{\rm e} &= -K\left[\xi'' + \frac{\xi'}{r} + \left(\vartheta'^2 + \frac{1}{r^2}\right)\sin\xi\cos\xi\right]\mathbf{n}_\parallel + K\left[\left(\vartheta'' + \frac{\vartheta'}{r}\right)\cos\xi - 2\xi'\vartheta'\sin\xi\right]\mathbf{n}_\perp,\\
\mathbf{K}_{\rm v} &= \left[\gamma_1\dot\xi - (\gamma_1 - \gamma_2\cos 2\xi)\cos\vartheta\,\frac{v_z'}{2} - \frac{\gamma_2}{4}\left(v_\varphi' - \frac{v_\varphi}{r}\right)\sin 2\xi\,\sin 2\vartheta\right]\mathbf{n}_\parallel\\
&\quad + \left[-\gamma_1\left(\dot\vartheta - \frac{v_\varphi}{r}\right)\cos\xi + \frac{\gamma_1 - \gamma_2\cos 2\vartheta}{2}\left(v_\varphi' - \frac{v_\varphi}{r}\right)\cos\xi + (\gamma_1+\gamma_2)\frac{v_z'}{2}\sin\xi\,\sin\vartheta\right]\mathbf{n}_\perp,\\
\mathbf{K}_{\rm s} &= \mathbf{n}\wedge\mathbf{H}_{\rm s} = \left(W_{{\rm s}z} - W_{{\rm s}r}\cos^2\vartheta\right)\sin\xi\cos\xi\,\mathbf{n}_\parallel + W_{{\rm s}r}\cos\xi\,\sin\vartheta\,\cos\vartheta\,\mathbf{n}_\perp.
\end{aligned}
$$

The balance of torques (2.3) requires:

$$
\begin{cases}
-K\left[\xi'' + \frac{\xi'}{r} + \left(\vartheta'^2 + \frac{1}{r^2}\right)\sin\xi\cos\xi\right] + \left(W_{{\rm s}z} - W_{{\rm s}r}\cos^2\vartheta\right)\sin\xi\cos\xi\\
\quad + \left[\gamma_1\dot\xi - (\gamma_1 - \gamma_2\cos 2\xi)\cos\vartheta\,\frac{v_z'}{2} - \frac{\gamma_2}{4}\left(v_\varphi' - \frac{v_\varphi}{r}\right)\sin 2\xi\,\sin 2\vartheta\right] = 0,\\
K\left[\left(\vartheta'' + \frac{\vartheta'}{r}\right)\cos\xi - 2\xi'\vartheta'\sin\xi\right] + W_{{\rm s}r}\cos\xi\,\sin\vartheta\,\cos\vartheta\\
\quad + \left[-\gamma_1\left(\dot\vartheta - \frac{v_\varphi}{r}\right)\cos\xi + \frac{\gamma_1 - \gamma_2\cos 2\vartheta}{2}\left(v_\varphi' - \frac{v_\varphi}{r}\right)\cos\xi + (\gamma_1+\gamma_2)\frac{v_z'}{2}\sin\xi\,\sin\vartheta\right] = 0.
\end{cases}
\tag{3.1}
$$

3.2. Balance of forces

If we use the same parametrization for the stress tensor (2.2), we obtain:

$$
\begin{aligned}
\mathbf{T}_{\rm e} &= -p\mathbf{I} - K\left[\left(\xi'^2 + \vartheta'^2\cos^2\xi\right)\mathbf{e}_r\otimes\mathbf{e}_r + \frac{\vartheta'}{r}\cos^2\xi\,(\mathbf{e}_r\otimes\mathbf{e}_\varphi + \mathbf{e}_\varphi\otimes\mathbf{e}_r)r + \frac{\cos^2\xi}{r^2}\,\mathbf{e}_\varphi\otimes\mathbf{e}_\varphi\right],\\
\mathbf{T}_{\rm v} &= \alpha_1\left[\cos\xi\,\sin\vartheta\left(v_\varphi' - \frac{v_\varphi}{r}\right) + \sin\xi\,v_z'\right]\cos\xi\,\cos\vartheta\,\mathbf{n}\otimes\mathbf{n}\\
&\quad + \left[\left(\dot\vartheta - \frac{v_\varphi}{r}\right)\cos\xi - \left(v_\varphi' - \frac{v_\varphi}{r}\right)\frac{\cos\xi}{2} - \frac{v_z}{2}\sin\xi\,\sin\vartheta\right](\alpha_2\,\mathbf{n}_\parallel\otimes\mathbf{n} + \alpha_3\,\mathbf{n}\otimes\mathbf{n}_\parallel)\\
&\quad + \left(\dot\xi - \frac{v_z}{2}\cos\vartheta\right)(\alpha_2\,\mathbf{n}_\perp\otimes\mathbf{n} + \alpha_3\,\mathbf{n}\otimes\mathbf{n}_\perp)\\
&\quad + \alpha_4\left[\frac{1}{2}\left(v_\varphi' - \frac{v_\varphi}{r}\right)(\mathbf{e}_\varphi\otimes\mathbf{e}_r + \mathbf{e}_r\otimes\mathbf{e}_\varphi) + \frac{v_z'}{2}(\mathbf{e}_z\otimes\mathbf{e}_r + \mathbf{e}_r\otimes\mathbf{e}_z)\right]\\
&\quad + \frac{1}{2}\left(v_\varphi' - \frac{v_\varphi}{r}\right)\cos\xi\left[\alpha_5(\sin\vartheta\,\mathbf{e}_r + \cos\vartheta\,\mathbf{e}_\varphi)\otimes\mathbf{n} + \alpha_6\,\mathbf{n}\otimes(\sin\vartheta\,\mathbf{e}_r + \cos\vartheta\,\mathbf{e}_\varphi)\right]\\
&\quad + \frac{v_z'}{2}\left[\alpha_5(\sin\xi\,\mathbf{e}_r + \cos\xi\cos\vartheta\,\mathbf{e}_z)\otimes\mathbf{n} + \alpha_6\,\mathbf{n}\otimes(\sin\xi\,\mathbf{e}_r + \cos\xi\cos\vartheta\,\mathbf{e}_z)\right],
\end{aligned}
$$

and

$$
\nabla W_{\rm s} = \frac{\partial W_{\rm s}}{\partial r}\,\mathbf{e}_r + \frac{\partial W_{\rm s}}{\partial(\mathbf{n}\cdot\mathbf{e}_r)}(\nabla\mathbf{e}_r)^{\rm T}\mathbf{n} = \left[\frac{W_{{\rm s}r}'}{2}\cos^2\xi\cos^2\vartheta + \frac{W_{{\rm s}z}'}{2}\sin^2\xi\right]\mathbf{e}_r + \frac{W_{{\rm s}r}}{r}\cos^2\xi\,\sin\vartheta\,\cos\vartheta\,\mathbf{e}_\varphi.
$$

For the reader's ease, we here recall that the divergence of a tensor, represented in cylindrical coordinates through

$$
\begin{aligned}
\mathbf{T} &= T_{rr}\,\mathbf{e}_r\otimes\mathbf{e}_r + T_{r\varphi}\,\mathbf{e}_r\otimes\mathbf{e}_\varphi + T_{rz}\,\mathbf{e}_r\otimes\mathbf{e}_z + T_{\varphi r}\,\mathbf{e}_\varphi\otimes\mathbf{e}_r + T_{\varphi\varphi}\,\mathbf{e}_\varphi\otimes\mathbf{e}_\varphi + T_{\varphi z}\,\mathbf{e}_\varphi\otimes\mathbf{e}_z\\
&\quad + T_{zr}\,\mathbf{e}_z\otimes\mathbf{e}_r + T_{z\varphi}\,\mathbf{e}_z\otimes\mathbf{e}_\varphi + T_{zz}\,\mathbf{e}_z\otimes\mathbf{e}_z,
\end{aligned}
$$

with components depending only on the radial coordinate r, is given by

$$
\operatorname{div}\mathbf{T} = \left(T_{rr}' + \frac{T_{rr} - T_{\varphi\varphi}}{r}\right)\mathbf{e}_r + \left(T_{\varphi r}' + \frac{T_{r\varphi} + T_{\varphi r}}{r}\right)\mathbf{e}_\varphi + \left(T_{zr}' + \frac{T_{zr}}{r}\right)\mathbf{e}_z.
$$

Thus, the radial component of the balance of forces (2.1) yields a differential equation which determines the hydrostatic pressure p, while the tangential and axial components complete, along with (3.1), a set of coupled motion equations for the unknowns ϑ, ξ, v_φ, and v_z:

$$\begin{cases} T'_{\varphi r} + \dfrac{T_{r\varphi} + T_{\varphi r}}{r} - \dfrac{W_{\mathrm{s}r}}{r} \cos^2\xi \sin\vartheta \cos\vartheta = 0, \\ T'_{zr} + \dfrac{T_{zr}}{r} = 0. \end{cases} \tag{3.2}$$

The second equation in (3.2) can be immediately integrated to give

$$T_{zr}(t,r) = \frac{A(t)}{r},$$

that is,

$$\begin{aligned} &\sin\xi\cos\xi\sin\vartheta\left[\frac{1}{2}\left(v'_\varphi - \frac{v_\varphi}{r}\right)\left(2\alpha_1\cos^2\xi\cos^2\vartheta + \alpha_3 + \alpha_6\right) - \left(\dot\vartheta - \frac{v_\varphi}{r}\right)\alpha_3\right] \\ &\quad + \frac{v'_z}{2}\left(\alpha_3\sin^2\xi\sin^2\vartheta + \alpha_4 + \alpha_5\cos^2\xi\cos^2\vartheta + \alpha_6\sin^2\xi\right) \\ &\quad + \left(\dot\xi - \frac{v_z}{2}\cos\vartheta\right)\cos\vartheta\left(\alpha_2\cos^2\xi - \alpha_3\sin^2\xi\right) = \frac{A(t)}{r}. \end{aligned} \tag{3.3}$$

On the contrary, Eq. $(3.2)_1$ cannot be integrated directly. Nevertheless, using $(3.1)_2$ to eliminate the boundary term W_{sr} from it, we can write it in the form

$$\psi' + 2\frac{\psi}{r} = 0 \quad \Rightarrow \quad \psi(t,r) = \frac{B(t)}{r^2}, \tag{3.4}$$

provided we define

$$\begin{aligned} \psi(t,r) :=\ & \frac{1}{2}\left(v'_\varphi - \frac{v_\varphi}{r}\right) \\ & \times\left[\cos^2\xi\left(2\alpha_1\cos^2\xi\cos^2\vartheta\sin^2\vartheta - \alpha_2\cos^2\vartheta + \alpha_3\sin^2\vartheta + \alpha_5\cos^2\vartheta + \alpha_6\sin^2\vartheta\right) + \alpha_4\right] \\ & + \left(\dot\vartheta - \frac{v_\varphi}{r}\right)\cos^2\xi\left(\alpha_2\cos^2\vartheta - \alpha_3\sin^2\vartheta\right) - \left(\dot\xi - \frac{v'_z}{2}\cos\vartheta\right)\sin\xi\cos\xi\sin\vartheta\cos\vartheta(\alpha_2+\alpha_3) \\ & + \frac{v'_z}{2}\sin\xi\cos\xi\sin\vartheta\left(2\alpha_1\cos^2\xi\cos^2\vartheta - \alpha_2\cos^2\vartheta + \alpha_3\sin^2\vartheta + \alpha_6\right). \end{aligned}$$

We will analyse Eqs. (3.3) and (3.4) in detail in the next section, but here we want to stress that their right-hand-side functions A and B, which are to be determined by imposing the appropriate boundary conditions, vanish in some common situations.

- If the nematic is bounded by a cylindrical surface where both strong anchoring and no-slip conditions are imposed, the velocity $\mathbf{v}$ and the time-derivatives $\dot\xi$ and $\dot\vartheta$ vanish at $\{r = R\}$ at all times. Thus, if we replace $r = R$ in both (3.3) and (3.4) we obtain $A = B \equiv 0\ \forall t$.
- If the nematic sample is much larger than the region in which the motion takes place, the macroscopic velocity and the time-derivatives in the left-hand side of (3.3) and (3.4) will be negligible far away from the distorsion, while the right-hand sides are forced to vanish as r^{-1} and r^{-2}, respectively. Thus, in this case, the large-r decay of the left-hand sides requires $A = B \equiv 0\ \forall t$ again.

In order to shorten our presentation, we will henceforth assume that either of the above assumptions holds, so that we can neglect both A and B, even if our results can be easily modified to take into account the general case.

3.3. Field equations

Eqs. $(3.1)_1$, $(3.1)_2$, (3.3), and (3.4) give a set of coupled differential equations for the molecular velocity and the director:

$$
\begin{cases}
\gamma_1 \dot{\xi} = K_\xi + \cos\vartheta\,(\gamma_1 - \gamma_2 \cos 2\xi)\,\dfrac{v_z'}{2} + \dfrac{\gamma_2}{4}\sin 2\xi \sin 2\vartheta\, \dfrac{\widetilde{v_\varphi'}}{2}, \\
\gamma_1 \cos\xi\, \widetilde{\dot{\vartheta}} = K_\vartheta + \cos\xi\,(\gamma_1 - \gamma_2\cos 2\vartheta)\,\dfrac{\widetilde{v_\varphi'}}{2} + (\gamma_1+\gamma_2)\sin\xi\sin\vartheta\,\dfrac{v_z'}{2}, \\
\cos^2\vartheta\; f(\xi)\,\dfrac{v_z'}{2} + \cos\vartheta\; g(\xi)\,\dot{\xi} + \sin^2\vartheta\,(\alpha_3\sin^2\xi + \alpha_4 + \alpha_6\sin^2\xi)\,\dfrac{v_z'}{2} \\
\quad + \sin\vartheta\sin\xi\cos\xi\left(g_2(\vartheta,\xi)\,\dfrac{\widetilde{v_\varphi'}}{2} - \alpha_3\,\widetilde{\dot{\vartheta}}\right) = 0, \\
\cos^2\xi\, f(\vartheta)\,\dfrac{\widetilde{v_\varphi'}}{2} + \cos^2\xi\, g(\vartheta)\,\widetilde{\dot{\vartheta}} + \sin^2\xi\,\big(\alpha_4 - \alpha_1\cos^2\xi\cos^2\vartheta\sin^2\vartheta\big)\,\dfrac{\widetilde{v_\varphi'}}{2} \\
\quad + \sin\vartheta\sin\xi\cos\xi\left(g_2(\vartheta,\xi)\,\dfrac{v_z'}{2} - (\alpha_2+\alpha_3)\cos\vartheta\,\dot{\xi}\right) = 0.
\end{cases}
\tag{3.5}
$$

In (3.5), f and g are the same functions already introduced in (1.4), that is:

$$f(\zeta) := 2\alpha_1 \sin^2\zeta\cos^2\zeta + \alpha_4 + (\alpha_5-\alpha_2)\cos^2\zeta + (\alpha_6+\alpha_3)\sin^2\zeta \quad \text{and}$$
$$g(\zeta) := \alpha_2\cos^2\zeta - \alpha_3\sin^2\zeta.$$

Furthermore, $g_2(\zeta,\chi) := 2\alpha_1\cos^2\zeta\cos^2\chi + \alpha_3 + \alpha_6$, and K_ξ, K_ϑ denote the components of the elastic and surface torques along the directions $\mathbf{n}_\parallel$ and $\mathbf{n}_\perp$:

$$
\begin{aligned}
K_\xi &:= K\left(\xi'' + \frac{\xi'}{r} + \frac{\sin\xi\cos\xi}{r^2}\right) + \left[K\,\vartheta'^2 + W_{\mathrm{s}r}\cos^2\vartheta - W_{\mathrm{s}z}\right]\sin\xi\cos\xi, \\
K_\vartheta &:= \left[K\left(\vartheta'' + \frac{\vartheta'}{r}\right) + W_{\mathrm{s}r}\sin\vartheta\cos\vartheta\right]\cos\xi - 2K\xi'\vartheta'\sin\xi.
\end{aligned}
\tag{3.6}
$$

Finally, $\widetilde{\dot{\vartheta}}$ and $\widetilde{v_\varphi'}$ stand for

$$\widetilde{\dot{\vartheta}} := \dot{\vartheta} - \frac{v_\varphi}{r} \quad \text{and} \quad \widetilde{v_\varphi'} := v_\varphi' - \frac{v_\varphi}{r}.$$

4. Cylindrical motions

Eqs. (3.5) are clearly unamenable for a complete analytical study. Nevertheless, it is useful to remark that they contain only two types of terms depending explicitly on the radial coordinate r. The static terms simply modify the elastic torques, and reflect the difference between cylindrical and planar equilibrium configurations. On the other hand, the dynamic terms explicitly depending on r are all multiplied by v_φ. They thus confirm that the structure of the motion equations feels the curved geometry only when the external normal varies along the macroscopic stream lines. To illustrate better this effect, we will now compare three different particular motions, obtained by requiring the director to lie in the planes orthogonal to the unit vectors $\mathbf{e}_r$, $\mathbf{e}_z$, and $\mathbf{e}_\varphi$, respectively.

4.1. Tangential-axial configurations ($\vartheta \equiv \pi/2$)

We begin by analysing the motions in which the director is everywhere orthogonal to $\mathbf{e}_r$. By $(3.5)_2$, $(3.5)_3$, and $(3.5)_4$, this type of configurations can be stable only in the absence of any nontrivial macroscopic motion, since the motion equations require $v_\varphi \equiv 0$ and $v_z' \equiv 0$. Thus, only a uniform drift along the z-direction would be compatible with configurations in which the director is always orthogonal to $\mathbf{e}_r$. Finally, Eq. $(3.5)_1$ trivially requires:

$$\gamma_1\dot{\xi} = K_\xi;$$

obviously, there are no back-flow effects since no flow is present.

4.2. Axial-radial configurations ($\vartheta \equiv 0$)

Let us now consider situations in which the director belongs to the plane determined by $\mathbf{e}_r$ and $\mathbf{e}_z$. The field equations $(3.5)_2$ and $(3.5)_4$ now imply $v_\varphi \equiv 0$ (independently of the boundary conditions), while $(3.5)_1$ and $(3.5)_3$ yield:

$$\dot{\xi} = \frac{K_\xi}{\gamma_{\mathrm{s}}(\xi)} \quad \text{and} \quad \frac{v_z'}{2} = \left(\frac{\gamma_1}{\gamma_{\mathrm{s}}(\xi)} - 1\right)\frac{K_\xi}{\gamma_1 - \gamma_2\cos 2\xi}. \tag{4.1}$$

Eqs. (4.1) exactly coincide with the planar equations of motion (1.2), with the same effective viscosity $\gamma_{\rm S}$ as in (1.3). This effect can be easily understood, since in this case the unit normal to the external surface does not vary along the stream lines of the fluid, which are parallel to $\mathbf{e}_z$. Thus, as in [15], back-flow effects just replace the viscosity γ_1 with the effective viscosity $\gamma_{\rm S}$, which depends on the director orientation.

4.3. Tangential-radial configurations ($\xi \equiv 0$)

Let us finally consider the most interesting case, that is when the director lies in the plane orthogonal to the z-direction, so that ϑ is the angle determined by the director $\mathbf{n}$ and $\mathbf{e}_r$. Eqs. $(3.5)_1$ and $(3.5)_3$ require $v_z' \equiv 0$. Thus, the vertical component of the molecular velocity must be constant. In particular, it vanishes if no-slip conditions are applied at the boundary or if the flow is supposed to vanish away from the boundary. The remaining equations $(3.5)_2$ and $(3.5)_4$ yield:

$$\dot\vartheta - \frac{v_\varphi}{r} = \frac{K_\vartheta}{\gamma_{\rm S}(\vartheta)} \quad \text{and} \quad \frac{1}{2}\left(v_\varphi' - \frac{v_\varphi}{r}\right) = \left(\frac{\gamma_1}{\gamma_{\rm S}(\vartheta)} - 1\right)\frac{K_\vartheta}{\gamma_1 - \gamma_2\cos 2\vartheta}. \tag{4.2}$$

Eqs. (4.2) have the same structure as (1.2). Nevertheless, in them v_φ' is replaced by $(v_\varphi' - v_\varphi/r)$ but, most important, $\dot\vartheta$ is replaced by $(\dot\vartheta - v_\varphi/r)$. Thus, it is not possible to obtain an evolution equation for the sole director, that is, independent of the macroscopic velocity. Clearly, the correction terms vanish if $r \to \infty$, since in that case the cylindrical symmetry tends to coincide with the planar symmetry for which Eqs. (1.2) and (1.3) were derived.

Eqs. (4.2) reveal that back-flow effects in the bulk cannot be taken into account by just introducing an effective viscosity. In fact, even when the elastic and surface torques are equilibrated ($K_\vartheta = 0$), Eq. $(4.2)_2$ does not forbid a macroscopic tangential flow, provided that $v_\varphi' = v_\varphi/r$. Then, by Eq. $(4.2)_1$, this flow creates a rotation of the director. This effect is peculiar of the curved geometry, since Eq. (1.2) shows that in a planar flow the macroscopic velocity and the variations of the director must be sustained by an elastic or a surface torque.

5. Surface dynamics

We now focus in the dynamics within the *boundary layer*, where the surface potential is concentrated. To this aim, we assume that the width h of the boundary layer is much smaller than the characteristic length of the system. In particular, $h \ll R$.

As soon as we spread the surface torques over the boundary layer, the actual boundary becomes a *free* surface, where the anchoring condition becomes $(\nabla\mathbf{n})\mathbf{e}_r = \mathbf{0}$, since $\mathbf{e}_r$ is parallel to the normal to the surface. In our cylindrical geometry this implies $\xi'(t,R) = \vartheta'(t,R) \equiv 0$ for all t. Thus, close to the external surface,

$$\xi(t,r) = \xi(t,R) + \frac{1}{2}\xi''(t,R)(r-R)^2 + \mathrm{o}\big((r-R)^2\big) \quad \text{and}$$
$$\vartheta(t,r) = \vartheta(t,R) + \frac{1}{2}\vartheta''(t,R)(r-R)^2 + \mathrm{o}\big((r-R)^2\big).$$

In the following we will use the notations $\xi_{\rm S}(t) := \xi(t,R)$ and $\vartheta_{\rm S}(t) := \vartheta(t,R)$ to denote the surface values of the angles ξ and ϑ. It is then allowed to assume that $\xi(t,r) \equiv \xi_{\rm S}(t)$ and $\vartheta(r,t) \equiv \vartheta_{\rm S}(t)$ in the whole boundary layer $r \in [R, R+h]$ provided that

$$\xi''(t,R) \ll \frac{1}{h^2} \quad \text{and} \quad \vartheta''(t,R) \ll \frac{1}{h^2}.$$

Analogously, and assuming the no-slip condition $v_z(t,R) = v_\varphi(t,R) \equiv 0$ to hold for all t, we expand the velocity components inside the slab

$$\begin{cases} v_z(t,r) = v_{{\rm S}z}(t)\dfrac{r-R}{h} + \dfrac{1}{2}v_z''(t,R)(r-R)^2 + \mathrm{o}\big((r-R)^2\big), \\ v_\varphi(t,r) = v_{{\rm S}\varphi}(t)\dfrac{r-R}{h} + \dfrac{1}{2}v_\varphi''(t,R)\,(r-R)^2 + \mathrm{o}\big((r-R)^2\big), \end{cases} \tag{5.1}$$

and we neglect the second order terms both in v_z and v_φ. In (5.1), $v_{{\rm S}z}$ and $v_{{\rm S}\varphi}$ denote the z- and φ-components of the molecular velocity computed at the end of the boundary layer, and not at the boundary (where $\mathbf{v} = \mathbf{0}$ by effect of the no-slip condition).

Let us now focus attention on the tangential-radial configurations, where the curvature effects can be better detected. Thus, we assume that $\xi \equiv 0$ and $v_z \equiv 0$, and we integrate $(4.2)_1$ over the cylindrical slab delimited by the boundary $\{r = R\}$ and the surface $\{r = R + h\}$. Considering $(3.6)_2$, and keeping only the leading order in which curvature effects can be defected, we arrive at:

$$h\left(\dot{\vartheta}_s - \frac{v_{s\varphi}}{2R}\right) = \frac{K\vartheta_s' + \mathbb{K}_s}{\gamma_s(\vartheta_s)}. \tag{5.2}$$

In (5.2), ϑ_s' denotes the radial derivative of the director direction computed at $r = R + h$, γ_s is the effective viscosity introduced in (1.3), and $\mathbb{K}_s$ is the total torque exerted by the boundary layer:

$$\int_R^{R+h} r\, H_s(r)\, \mathrm{d}r =: \mathbb{K}_s(R+h).$$

The factor $1/2$ which multiplies the tangential velocity in (5.2) comes from the fact that we are assuming that ϑ_s is almost constant throughout the boundary layer, while the tangential velocity is null at the surface $\{r = R\}$ and equal to $v_{s\varphi}$ at $\{r = R + h\}$.

Similarly, if we integrate $(4.2)_2$ over the boundary layer, the leading order yields:

$$\frac{v_{s\varphi}}{2} = \left(\frac{\gamma_1}{\gamma_s(\vartheta_s)} - 1\right)\frac{K\vartheta_s' + \mathbb{K}_s}{\gamma_1 - \gamma_2\cos 2\vartheta_s}. \tag{5.3}$$

Finally, if we use (5.3) to eliminate the velocity from (5.2), we arrive at:

$$h\gamma_s(\vartheta_s)\left(1 + \frac{g(\vartheta_s)}{f(\vartheta_s)}\,\frac{h}{R} + \mathcal{O}\left(\frac{h}{R}\right)^2\right)\dot{\vartheta}_s = K\vartheta_s' + \mathbb{K}_s, \tag{5.4}$$

where f and g are defined as in (1.4).

5.1. *Effective viscosity in cylindrical flows*

Eq. (5.4) has the same structure of (1.1), provided we replace in this latter γ_s by

$$\widetilde{\gamma}_s(\vartheta) = \gamma_s(\vartheta)\left(1 + \frac{g(\vartheta)}{f(\vartheta)}\,\frac{h}{R} + \mathcal{O}\left(\frac{h}{R}\right)^2\right). \tag{5.5}$$

Thus, the curvature of the external surface modifies the effective viscosity. The sign of the leading order of this correction depends on both the concavity of the surface and on Leslie's coefficients. The former determines the sign of h: $h > 0$ if the fluid flows outside the cylindrical surface, while h must be taken negative if the nematic occupies the inner side of the cylinder.

On the other hand, the sign of the ratio g/f depends only on g. In fact, by using dissipation arguments it is possible to prove [3,15] that $f(\vartheta)$ must be strictly positive for all values of ϑ. Thus, and since $g(\vartheta) = \alpha_2\cos^2\vartheta - \alpha_3\sin^2\vartheta$, the sign of g/f depends only on the relative signs of the Leslie coefficients α_2 and α_3.

- If $\alpha_2/\alpha_3 > 0$, we can introduce the critical angle $\vartheta_* := \arctan\sqrt{\alpha_2/\alpha_3} \in (0, \pi/2)$. The ratio g/f has the same sign of α_2 and α_3 when $\vartheta \in [0, \vartheta_*) \cup (\pi - \vartheta_*, \pi]$, and the opposite sign otherwise, with $g(\vartheta_*) = g(\pi - \vartheta_*) = 0$.
- If $\alpha_2/\alpha_3 < 0$, the ratio g/f shares the same sign as α_2.
- If α_2 is null, g/f has the opposite sign with respect to α_3, with $g(0) = g(\pi) = 0$.
- If α_3 is null, g/f has the same sign of α_2, with $g(\pi/2) = 0$.
- Clearly, g/f vanishes if both α_2 and α_3 do so.

We remark that for materials that align in shear and satisfy Parodi's relation $\alpha_6 - \alpha_5 = \alpha_2 + \alpha_3$ [22], it holds $\alpha_2 \leqslant \alpha_3 < 0$ [23, 24]. These materials have a positive ratio α_2/α_3, and thus also a critical angle of the director in which the curvature correction of the effective viscosity changes sign. Furthermore, it has been recently proven that the degeneracy of the ratio α_2/α_3 is deeply related with the onset of defects in Poiseuille nematic flows [25].

To conclude this section, and in order to give a quantitative idea of how the ratio g/f depends on ϑ, we consider the following expressions for the Leslie coefficients, first derived by Marrucci [26,27] and widely used thenceforth [28–30,25]:

$$\alpha_1 = -s^2 k(s), \qquad \alpha_2 = -\frac{s(1+2s)}{2+s}k(s), \qquad \alpha_3 = -\frac{s(1-s)}{2+s}k(s), \qquad \alpha_4 = \frac{1-s}{3}k(s), \qquad \alpha_5 = sk(s),$$
$$\alpha_6 = 0. \tag{5.6}$$

In (5.6), s denotes the *degree of orientation* [31] of the nematic liquid crystal, $k(s) := \eta_0\,(1 - s^2)^2$, and η_0 is related to the isotropic viscosity of the flow [32,31]. We remark that any nematic liquid crystal that satisfies (5.6) possesses a non-symmetric stress tensor. In fact, as we have already underlined in Section 2, the stress tensor is symmetric only if both $\alpha_2 = \alpha_3$ and $\alpha_5 = \alpha_6$, but (5.6) shows that these requirements are satisfied only when $s = 0$, i.e., in the isotropic phase.

If we replace (5.6) in (1.4) we obtain:

$$f(\vartheta) = \frac{8 + 8s + 14s^2 - 3s^3 + 12s(2+s)\cos 2\vartheta + 3s^2(2+s)\cos 4\vartheta}{12(2+s)} \quad \text{and} \tag{5.7}$$

$$g(\vartheta) = -\frac{s(3s + (2+s)\cos 2\vartheta)}{12(2+s)}, \tag{5.8}$$

so that

$$\frac{g(\vartheta)}{f(\vartheta)} = -\frac{6s(3s + (2+s)\cos 2\vartheta)}{8 + 8s + 14s^2 - 3s^3 + 12s(2+s)\cos 2\vartheta + 3s^2(2+s)\cos 4\vartheta}.$$

By analysing the sign of $(5.8)_1$, it is easy to prove that the dissipation condition $f(\vartheta) > 0\ \forall\vartheta$ holds for all values of the degree of orientation $s \in (-1/2, 1)$, but the extremes $s = 1$ (where $f(\vartheta) = 2\cos^4\vartheta$ vanishes if $\vartheta = \pi/2$) and $s = -1/2$ (where $f(\vartheta) = 1/(3 - \cos 2\vartheta)\sin^2\vartheta$ vanishes if $\vartheta = 0$). Furthermore, from $(5.6)_2$ and $(5.6)_3$ we find that

$$\frac{\alpha_2}{\alpha_3} = \frac{1+2s}{1-s} > 0 \quad \forall s \in \left(-\frac{1}{2}, 1\right).$$

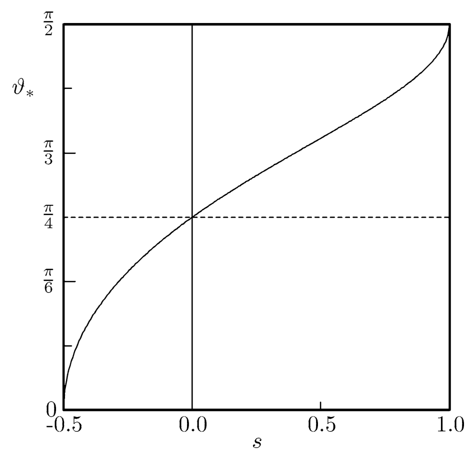

Fig. 2. Dependence of the critical angle ϑ_* on the degree of orientation s. For materials that align in shear, the ratio g/f has the sign of the Leslie coefficients α_2, α_3 when $\vartheta \in [0, \vartheta_*) \cup (\pi - \vartheta_*, \pi]$, and the opposite sign otherwise, with $g(\vartheta_*) = g(\pi - \vartheta_*) = 0$.

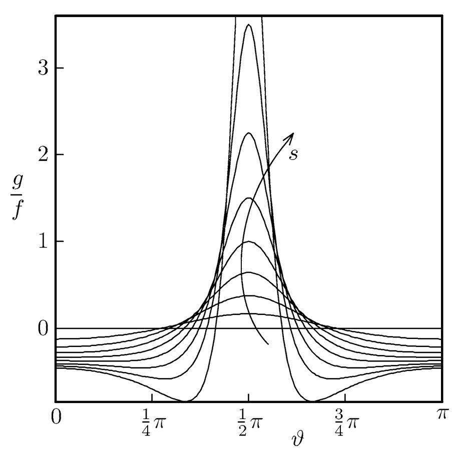

Fig. 3. Correction g/f of the effective viscosity as a function the angle ϑ between $\mathbf{n}$ and $\mathbf{e}_r$, when the Leslie coefficients $\{\alpha_1, \ldots, \alpha_6\}$ are chosen as in (5.6). The degree of orientation s attains the values 0.1, 0.2, 0.3, 0.4, 0.5, 0.6, 0.7, and 0.8.

Thus, there exists a critical angle ϑ_*, given by $\vartheta_* = \arctan\sqrt{\frac{1+2s}{1-s}}$, where the correction of the effective viscosity changes sign. Fig. 2 shows that ϑ_* increases monotonically with s: it tends to 0 when $s \to -1/2$, attains the value $\pi/4$ when $s = 0$, and approaches $\pi/2$ when $s \to 1$.

Finally, Fig. 3 shows how g/f depends on ϑ for different values of the degree of orientation s: g/f is maximum when $\vartheta = \pi/2$ (planar anchoring), with a peak which diverges when $s \to 1$. Clearly, the curvature effects vanish when $s \to 0$, i.e., close to the nematic-isotropic transition.

6. Conclusions

In this paper, we have analysed the flow of a nematic liquid crystal bounded by a cylindrical surface, which induces both translational and axial symmetry. Curvature effects are more tangible when both the director and the macroscopic velocity of the nematic molecules are orthogonal to the axis of the cylinder. When this is the case, it is not possible to obtain a bulk motion equation for the sole director, since even in the absence of elastic or surface torques a macroscopic velocity may induce a director rotation.

Nevertheless, we have shown that the phenomenological boundary condition (1.1) can be applied to describe also a nematic liquid crystal flowing close to a curved surface. However, it is necessary to replace in it $\gamma_{\rm S}$ with the effective viscosity $\widetilde{\gamma}_{\rm S}$ introduced in (5.5).

Eq. (5.5) shows that $\widetilde{\gamma}_{\rm S}$ may be greater or smaller than $\gamma_{\rm S}$, depending on the concavity of the external surface and the director direction. More precisely, we have shown that in materials that align in shear it exists a critical angle ϑ_* across which the curvature correction to the surface viscosity changes sign. Fig. 2 shows how ϑ_* depends on the degree of orientation of the nematic when Marrucci's expressions are used for the Leslie coefficients. Finally, Fig. 3 shows that, depending on the degree of orientation, the curvature correction is maximum when the surface director is tangent to the boundary.

We conclude by remarking that, besides the curvature of the boundary, there are other factors that may influence the effective viscosity in nematic flows. Among them, a key rôle should be played by the biaxial layer induced by the surface in the otherwise uniaxial nematic [33]. The dynamical theory of biaxial nematic liquid crystals [34,35] allows in principle to repeat the analysis here performed to account for biaxial effects. However, these latter are expected to be most tangible during transient regimes [36].

Acknowledgements

I gratefully acknowledge Epifanio G. Virga for useful discussions and comments on these topics. I also thank an anonymous referee for his suggestions.

References

[1] J.L. Ericksen, Conservation laws for liquid crystals, Trans. Soc. Rheol. 5 (1961) 23–34.
[2] J.L. Ericksen, Inequalities in liquid crystals theory, Phys. Fluids 9 (1966) 1205–1207.
[3] F.M. Leslie, Some constitutive equations for liquid crystals, Arch. Ration. Mech. Anal. 28 (1968) 265–283.
[4] A. Rapini, M. Papoular, Distorsion d'une lamelle nématique sous champ magnétique. Conditions d'ancrage aux parois, J. Phys. Coll. C4 30 (1969) 54–56.
[5] S. Pikin, G. Ryschenkow, W. Urbach, On new type of electrohydrodynamics instability in tilted nematic layers, J. Phys. 37 (1976) 241–244.
[6] A.I. Derzhanski, A.G. Petrov, Flexoelectricity in nematic liquid crystals, Acta Phys. Pol. A 55 (1979) 747–767.
[7] A.D. Rey, Periodic textures of nematic polymers and orientational slip, Macromol. 24 (1991) 4450–4456.
[8] A. Gharbi, F.R. Fekih, G.E. Durand, Dynamics of surface anchoring breaking in a nematic liquid crystal, Liq. Cryst. 12 (1992) 515–520.
[9] J. Stelzer, R. Hirning, H.-R. Trebin, Influence of surface anchoring and viscosity upon the switching behaviour of twisted nematic cells, J. Appl. Phys. 74 (1993) 6046–6052.
[10] P.J. Kedney, F.M. Leslie, Switching in a simple bistable nematic cell, Liq. Cryst. 24 (1998) 613–618.
[11] J.G. McIntosh, F.M. Leslie, Flow induced surface switching in a bistable nematic device, J. Engrg. Math. 37 (2000) 129–142.
[12] A. Mertelj, M. Čopič, Surface-dominated orientational dynamics and surface viscosity in confined liquid crystals, Phys. Rev. Lett. 81 (1998) 5844–5847.
[13] I. Dozov, M. Nobili, G.E. Durand, Fast bistable nematic display using monostable surface switching, Appl. Phys. Lett. 70 (1997) 1179–1181.
[14] I. Dozov, G.E. Durand, Surface controlled nematic bistability, Liq. Cryst. Today 8 (1998) 1–7.
[15] G.E. Durand, E.G. Virga, Hydrodynamic model for surface nematic viscosity, Phys. Rev. E 59 (1999) 4137–4142.
[16] C.Z. Van Doorn, Transient behaviour of a twisted nematic liquid-crystal in an electric field, J. Phys. Coll. C1 36 (1975) 261–263.

[17] A.F. Martins, P. Esnault, F. Volino, Measurement of the viscoelastic coefficients of main-chain nematic polymers by an NMR technique, Phys. Rev. Lett. 57 (1986) 1745–1748.
[18] F.C. Frank, On the theory of liquid crystals, Discuss. Faraday Soc. 25 (1958) 19–28.
[19] A. Sonnet, E.G. Virga, Dilution of nematic surface potentials: Statics, Phys. Rev. E 61 (2000) 5401–5406.
[20] A. Sonnet, E.G. Virga, G.E. Durand, Dilution of nematic surface potentials: Relaxation dynamics, Phys. Rev. E 62 (2000) 3694–3701.
[21] R. Hirning, W. Funk, H.-R. Trebin, M. Schmidt, H. Schmiedel, Threshold behavior and electro-optical properties of twisted nematic layers with weak anchoring in the tilt and twist angle, J. Appl. Phys. 70 (1991) 4211–4216.
[22] O. Parodi, Stress tensor for a nematic liquid crystal, J. Phys. 31 (1970) 581–584.
[23] P.K. Currie, G.P. MacSithigh, The stability and dissipation of solutions for shearing flow of nematic liquid crystals, J. Mech. Appl. Math. 32 (1979) 499–511.
[24] J.G. McIntosh, F.M. Leslie, D.M. Sloan, Stability for shearing flow of nematic liquid crystals, Contin. Mech. Thermodyn. 9 (1997) 293–308.
[25] M.C. Calderer, C. Liu, Poiseuille flow of nematic liquid crystals, Internat. J. Engrg. Sci. 38 (2000) 1007–1022.
[26] G. Marrucci, Prediction of Leslie coefficients for rodlike polymer nematics, Mol. Cryst. Liq. Cryst. 72 (1981) 153–161.
[27] G. Marrucci, P.L. Maffettone, Description of the liquid crystalline phase of rodlike polymers at high shear rates, Macromol. 22 (1989) 4076–4082.
[28] R.G. Larson, Roll-cell instability in shearing flows of nematic polymers, J. Rheology 37 (1993) 175–197.
[29] H.W. Han, A.D. Rey, Simulation and validation of temperature effects on the nematorheology of aligning and non-aligning liquid crystals, J. Rheology 39 (1995) 301–322.
[30] M.C. Calderer, C. Liu, Liquid crystal flow: dynamic and static configurations, SIAM J. Appl. Math. 60 (2000) 1925–1949.
[31] J.L. Ericksen, Liquid crystals with variable degree of orientation, Arch. Rational Mech. Anal. 113 (1991) 97–120.
[32] N. Kuzuu, M. Doi, Constitutive equation for nematic liquid crystals under weak velocity gradient derived from a molecular kinetic equation, J. Phys. Soc. Japan 52 (1983) 3486–3494.
[33] P. Biscari, E.G. Virga, Local stability of biaxial nematic phases between two cylinders, Internat. J. Nonlinear Mech. 32 (1997) 337–351.
[34] F.M. Leslie, J.S. Laverty, T. Carlsson, Continuum theory for biaxial nematic liquid crystals, Quart. J. Mech. Appl. Math. 45 (1992) 595–606.
[35] M. Kröger, S. Sellers, Fokker–Planck calculations of the viscosities of biaxial fluids, Phys. Rev. E 56 (1997) 1804–1807.
[36] P.L. Maffettone, A.M. Sonnet, E.G. Virga, Shear-induced biaxiality in nematic polymers, J. Non-Newtonian Fluid Mech. 90 (2000) 283–297.